Use of the Moment Method and Dyadic Green's Functions in the Analysis of Quasi-Optical Structures

T. W. Nuteson†, G. P. Monahan†, M. B. Steer†, K. Naishadham*, J. W. Mink†, and F. K. Schwering◇

† Electronics Research Laboratory, Department of Electrical and Computer Engineering, North Carolina State University, Raleigh, NC 27695-7911

* Department of Electrical Engineering, Wright State University, Dayton, OH 45435

◇ CECOM, Attn. AMSEL-RD-ST-C, Ft. Monmouth, NJ 07703-5203

Abstract. A moment method using a dyadic Green's function is developed for the analysis of quasi-optical systems. The dyadic Green's function used has separate terms for the paraxial and non-paraxial fields and is much easier to develop than a mixed potential Green's function. The method is applied to the analysis of antenna elements in a quasi-optical resonator.

1. Introduction

Quasi-optical techniques provide a means for combining power from numerous solid-state millimeter-wave sources attached to radiating elements such as antenna arrays or grids, as is shown in Figs. 1 and 2. The power from the radiating elements is combined in free-space over a distance of many wavelengths to channel power predominately into a single paraxial mode. The complex device field interactions render it difficult to optimize efficiencies and ensure stable operation. However, computer aided analysis techniques are evolving to aid in design. The strategy is to develop, using numerical field analysis, a multiport impedance model of the linear part of the quasi-optical system. This can then be interfaced with commercial microwave circuit simulators. Efficiency requires that volumetric discretization must be avoided. By utilizing Green's functions appropriate to the physical background, discretization can be limited to surfaces. In [1-3] a series of developments culminated in a straight forward methodology for developing the dyadic Green's function of a quasi-optical structure. The dyadic Green's function is derived by separately considering paraxial and non-paraxial modes. It is not feasible to derive a mixed, scalar and vector, potential Green's function, as required in conventional space domain moment method techniques. Alternatively, we have adapted an efficient moment method field solver [4,5] to use dyadic Green's functions. In this paper we introduce for the first time a moment method technique using a dyadic Green's function which describes all of the electric fields, both cavity coupled and free space, for radiating elements of arbitrary shape in an open cavity resonator. Unlike the work in [6] which is applicable only to infinite periodic quasi-optical structures, this work is applicable to structures of finite extent.

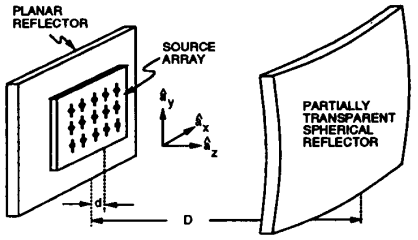

Figure 1: Quasi-optical power combiner configuration.

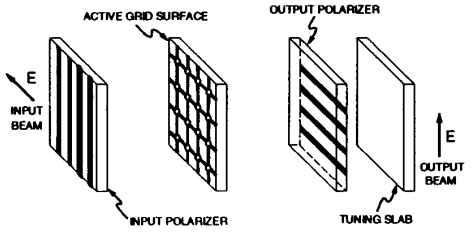

Figure 2: A grid amplifier on a dielectric slab with X and Y polarizers.

WE 4B

2. Quasi-Optical Resonator Dyadic Green's Function

A dyadic Green's function for a quasi-optical resonator was developed by Heron et al. [2, 3]. The resonator, shown in Fig. 1, consists of a planar reflector at $z = 0$ and a partially transmitting spherical reflector

CH3577-4/95/0000-0913$01.00 © 1995 IEEE

with its center located at $z = D$. The planar reflector is assumed to be perfectly conducting with infinite dimensions in the transverse direction. The spherical reflector is of finite dimension with radii of curvature along the x and y axis, F_x and F_y, respectively. The medium in the cavity is free space. The Green's function of the resonator can be divided into two parts

$$\bar{\bar{\mathbf{G}}}_E = \bar{\bar{\mathbf{G}}}_{Ec} + \bar{\bar{\mathbf{G}}}_{Eh} \tag{1}$$

where $\bar{\bar{\mathbf{G}}}_{Ec}$ and $\bar{\bar{\mathbf{G}}}_{Eh}$ are the cavity and half-space contributions, respectively. The cavity Green's function describes the coupling between an electric current source above the planar reflector, $z = d$, and all of the electric fields within the cavity, both resonant cavity modal fields and a correction to the half-space Green's function to account for these cavity fields. The $\hat{\mathbf{a}}_x\hat{\mathbf{a}}_x$ component is given as

$$G^{xx}_{Ec} = -\sum_{m=0}^{N_m}\sum_{n=0}^{N_n} \frac{R_{mn}\psi_{mn}}{2\left(1+R_{mn}\psi_{mn}\right)}\left(E^-_{mn}-E^+_{mn}\right) \cdot\left(\acute{E}^-_{mn}-\acute{E}^+_{mn}\right),\ 0<z\le D \tag{2}$$

where N_m and N_n represent the number of transverse modes. The reader is referred to [2,3] for the expressions of E_{mn}, R_{mn}, and ψ_{mn}. The half-space is defined as the region, $z > 0$, with the absence of the spherical reflector. The dyadic Green's function for the half-space exhibits a strong singularity in the self-terms. For this reason it is desirable to work in the spectral domain. The $\hat{\mathbf{a}}_x\hat{\mathbf{a}}_x$ component, for $0 < z \le d$, in the spectral domain is given as [7]

$$\tilde{G}^{xx}_{Eh}(k_x,k_y) = \frac{-Z_0}{2k_0}\left(\frac{k_0^2-k_x^2}{k_z}\right)\left(1-e^{-j2dk_z}\right) \tag{3}$$

where

$$k_z^2 = k_0^2 - k_x^2 - k_y^2\ ,\ \ \mathrm{Im}(k_z) < 0 \tag{4}$$

and Z_0 and k_0 are the free space impedance and wavenumber, respectively. The imaginary part of k_z needs to be less than zero in order to satisfy the radiation condition. The spectral domain Green's function for half-space does not exhibit any singularities.

3. Method Of Moments

The boundary value problem for the current distribution on the conductor surface, located at $z = d$, is formulated as an electric field integral equation. The patch antenna surface is segmented into equal size rectangular cells of dimension $a \times b$ and sinusoidal basis functions are used for expansion and testing (Galerkin method), resulting in a set of linear equations,

$$[\mathbf{Z}][\mathbf{I}] = [\mathbf{V}] \tag{5}$$

to be solved for the unknown currents I_n. The terms of the moment matrix $[\mathbf{Z}]$ can be divided into

$$Z_{ji} = Z_{c,ji} + Z_{h,ji} \tag{6}$$

where Z_c and Z_h represent the cavity and half-space contributions, respectively, given by

$$\begin{aligned} Z^{xx}_{c,ji} = &\sum_{m=0}^{N_m}\sum_{n=0}^{N_n}\frac{R_{mn}\psi_{mn}}{2\left(1+R_{mn}\psi_{mn}\right)} \cdot\int_{y_j-\frac{b}{2}}^{y_j+\frac{b}{2}}\int_{x_j-a}^{x_j+a} J^x_j(x) \cdot\left[E^-_{mn}(x,y,d)-E^+_{mn}(x,y,d)\right]dx\,dy \\ &\cdot\int_{y_i-\frac{b}{2}}^{y_i+\frac{b}{2}}\int_{x_i-a}^{x_i+a} J^x_i(x') \cdot\left[E^-_{mn}(x',y',d)-E^+_{mn}(x',y',d)\right]dx'dy' \end{aligned} \tag{7}$$

$$Z^{xx}_{h,ji} = \frac{-1}{\pi^2}\int_0^{\pi/2}\int_0^{\infty}\tilde{G}^{xx}_{Eh}(k_x,k_y) \cdot\tilde{J}^x_j(k_x,k_y)^*\,\tilde{J}^x_i(k_x,k_y)\,\beta\,d\beta\,d\alpha \tag{8}$$

where

$$J^x_i(x) = \frac{1}{b}\frac{\sin\left[k_0\left(a-|x-x_i|\right)\right]}{\sin(k_0a)}\ ,\quad \text{for } |x-x_i|\le a\ ,\ \ |y-y_i|\le\frac{b}{2} \tag{9}$$

$$\tilde{J}^x_i(k_x,k_y) = \int_{y_i-\frac{b}{2}}^{y_i+\frac{b}{2}}\int_{x_i-a}^{x_i+a} J^x_i(x) \cdot e^{-jk_xx}e^{-jk_yy}\,dx\,dy \tag{10}$$

The x-directed sinusoidal basis function J^x_i is spanned over two rectangular cells, centered at (x_i, y_i), and is constant in the y direction. $\tilde{J}^x_i$ is the two dimensional Fourier transform of J^x_i and can be evaluated in closed form. The $(*)$ represents the complex conjugate. Primed coordinates denote the source location and unprimed coordinates denote the test location. The cavity moment matrix elements in (7) contain no singularities and have separable source and test fields which allows for efficient evaluation in the spatial domain. The half-space moment matrix elements in (8) are computed in the spectral domain [7] to avoid the singularity in the spatial domain half-space Green's functions. A transformation to polar coordinates, where $k_x = \beta\cos\alpha$ and $k_y = \beta\sin\alpha$, is used to reduce the number of infinite integrations.

For this formulation only a single row of cell subdivision is considered. A delta-gap voltage generator is used as the excitation vector [V], given as

$$V_p = \begin{cases} 1 & \text{for } p \text{ equal to feed point} \\ 0 & \text{otherwise} \end{cases} \tag{11}$$

The input impedance at the location of the delta-gap voltage generator is computed as

$$Z_{in} = \frac{V_p}{I_p} \tag{12}$$

where I_p is the current at the delta-gap computed by the method of moments.

4. Comparison Of Computed And Experimental Results

The radii of curvature of the spherical reflector are $F_x = 0.894308$ m, $F_y = 0.953839$ m and its location is $D = 0.620494$ m. The resonant frequencies of the cavity are given as [2]

$$f_{m,n,q} = \frac{c}{2D}\left[q + \frac{1}{\pi}\left(m+\frac{1}{2}\right)\tan^{-1}\sqrt{\frac{D}{2F_x - D}} + \frac{1}{\pi}\left(n+\frac{1}{2}\right)\tan^{-1}\sqrt{\frac{D}{2F_y - D}}\right] \quad (13)$$

where c is the speed of light and q is the longitudinal mode number corresponding to an integer number of longitudinal half waves. For the $q = 35$ family, measurements were made using an electrically short inverted L antenna, shown in Fig. 3, with a wire diameter of 0.9 mm and a length $L = 2.6$ mm. The L antenna was divided into 10 cells with a delta-gap source placed between the first and second cells. The location of the antenna in the cavity was at (-90.6 mm, 15 mm) with $d = 1.9$ mm. The magnitude and phase of the input impedance is shown in Figs. 4 and 5 for the $\mathrm{TEM}_{0,0,35}$ mode and in Figs. 6 and 7 for the $\mathrm{TEM}_{0,1,35}$ and $\mathrm{TEM}_{1,0,35}$ modes.

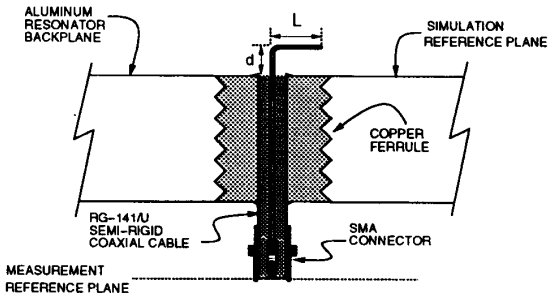

Figure 3: A coaxial fed inverted L antenna.

A measurement of a coaxial center fed patch antenna with dimension $L = 15$ mm and $W = 5$ mm, was taken without the reflector at $d = 1$ mm. The input impedance is shown in Fig. 8. The patch was divided into 16 cells with a delta-gap source placed in the center. Fig. 9 shows the simulated results for the $\mathrm{TEM}_{0,0,23}$ and $\mathrm{TEM}_{0,0,34}$ modes for a patch antenna in the cavity located at (30 mm, 30 mm). The Q, computed as $f/\Delta f$, was found to be 11,200 and 15,020 for the $\mathrm{TEM}_{0,0,23}$ and $\mathrm{TEM}_{0,0,34}$ modes, respectively.

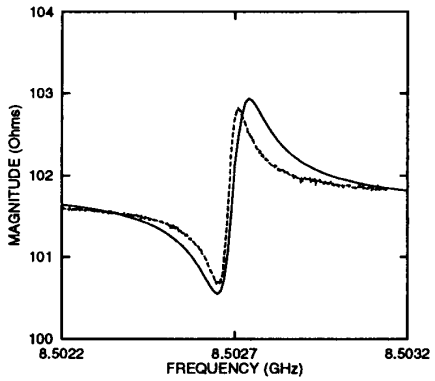

Figure 4: Input impedance magnitude of the L antenna for the $\mathrm{TEM}_{0,0,35}$ mode: solid line, simulation; dashed line, measurement.

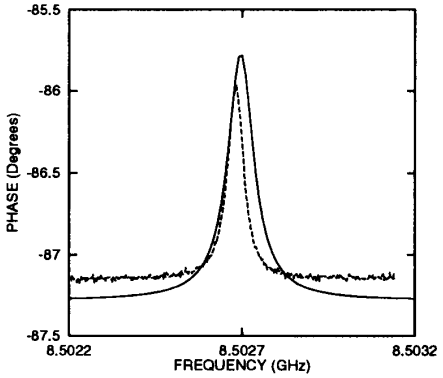

Figure 5: Input impedance phase of the L antenna for the $\mathrm{TEM}_{0,0,35}$ mode: solid line, simulation; dashed line, measurement.

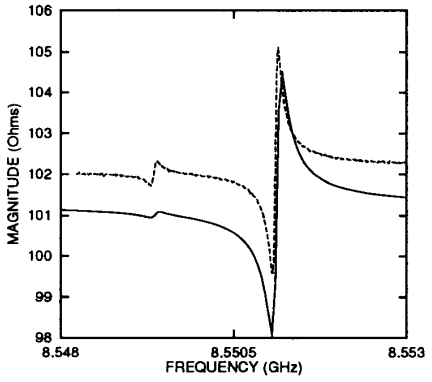

Figure 6: Input impedance magnitude of the L antenna for the $\mathrm{TEM}_{0,1,35}$ mode (left) and $\mathrm{TEM}_{1,0,35}$ mode (right): solid line, simulation; dashed line, measurement.

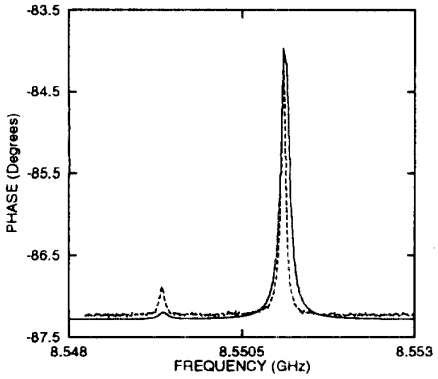

Figure 7: Input impedance phase of the L antenna for the $TEM_{0,1,35}$ mode (left) and $TEM_{1,0,35}$ mode (right): solid line, simulation; dashed line, measurement.

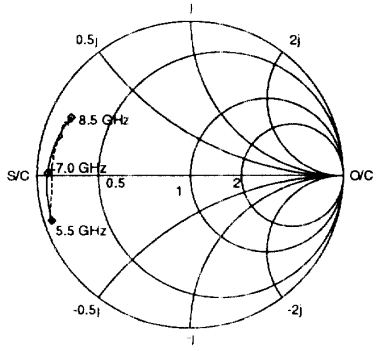

Figure 8: Impedance Smith chart showing the input impedance of the patch antenna without the reflector: solid line, simulation; dashed line, measurement.

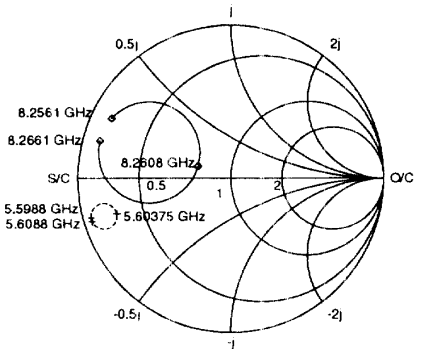

Figure 9: Impedance Smith chart showing the input impedance of the simulated input impedance of the patch antenna in the cavity: solid line, $TEM_{0,0,34}$ mode; dashed line, $TEM_{0,0,23}$ mode.

5. Conclusions

A moment method implementation has been developed for the analysis of antenna elements in a quasi-optical resonator. The antennas can be of arbitrary shape and size. The moment matrix elements are computed using a combination of spatial and spectral domains. Simulated results have been shown to compare favorably with measurements. The technique presented here will aid in the design of quasi-optical systems by accurately predicting the impedances of the radiating elements used in quasi-optics. Work continues in the development of quasi-optical Green's functions of grid amplifiers and polarizers.

Acknowledgment

This work was supported in part by the U.S. Army Research Office through grant DAAL03-89-G-0030.

References

[1] J. W. Mink, "Quasi-optical power combining of solid-state millimeter-wave sources," *IEEE Trans. Microwave Theory Tech.*, vol. MTT-34, pp. 273-279, Feb. 1986.

[2] P. L. Heron, G. P. Monahan, J. W. Mink, F. K. Schwering, and M. B. Steer, "Impedance matrix of an antenna array in a quasi-optical resonator," *IEEE Trans. Microwave Theory Tech.*, vol. MTT-41, pp. 1816-1826, Oct. 1993.

[3] P. L. Heron, F. K. Schwering, G. P. Monahan, J. W. Mink, and M. B. Steer, "A dyadic Green's function for the plano-concave quasi-optical resonator," *IEEE Microwave Guided Wave Lett.*, vol. 3, pp. 256-258, Aug. 1993.

[4] K. Naishadham and T. W. Nuteson, "Efficient analysis of passive microstrip elements in MMICs," *Int. Journal Microwave and Millimeter-Wave Computer-Aided Eng.*, vol. 4, pp. 219-229, July 1994.

[5] T. W. Nuteson, K. Naishadham, and R. Mittra, "Spatial interpolation of the moment matrix for efficient analysis of microstrip circuits," *IEEE Microwave Theory Tech. Int. Symp.*, Atlanta, GA, pp. 971-974, June 1993.

[6] S. C. Bundy and Z. B. Popović, "A generalized analysis for grid oscillator design," *IEEE Trans. Microwave Theory Tech.*, vol. MTT-42, pp. 2486-2491, Dec. 1994.

[7] D. M. Pozar, "Analysis and design considerations for printed phased-array antennas," in *Handbook of Microstrip Antennas*, J. R. James and P. S. Hall (ed.), London: Peter Peregrinus Ltd., pp. 693-753, 1989.